A theoretical study on the frequency-dependent electric conductivity of electrolyte solutions. II. Effect of hydrodynamic interaction

T. Yamaguchi,[a] T. Matsuoka, and S. Koda
Department of Molecular Design and Engineering, Graduate School of Engineering, Nagoya University, Furo-cho B2-3(611), Chikusa, Nagoya, Aichi 464-8603, Japan

(Received 27 May 2008; accepted 29 January 2009; published online 6 March 2009)

The theory on the frequency-dependent electric conductivity of electrolyte solutions proposed previously by Yamaguchi *et al.* [J. Chem. Phys. **127**, 234501 (2007)] is extended to include the hydrodynamic interaction between ions. The theory is applied to the aqueous solution of NaCl and the concentration dependence of the conductivity agrees well with that determined by experiments. The effects of the hydrodynamic and relaxation effects are highly nonadditive in the concentrated solution, because the hydrodynamic interaction between ions affects the time-dependent response of the ionic atmosphere. The decrease in the electric conductivity is divided into the contributions of ion pair distribution at various distances. The long-range ionic atmosphere plays a major role at the concentration as low as 0.01 mol/kg, whereas the contribution of the contact ion pair region is important at 1 mol/kg. The magnitude of the contribution of the contact ion pair region is scarcely dependent on the presence of the hydrodynamic interaction. The transport number of cation is calculated to be a decreasing function of concentration as is observed in experiments. © *2009 American Institute of Physics*. [DOI: 10.1063/1.3085717]

I. INTRODUCTION

The concentration dependence of the electric conductivity of electrolyte solutions has been one of the most important problems in the physical chemistry of electrolyte solutions, so that a large number of studies has been performed on it.[1–15] In the low-concentration region, there are two factors, called the electrophoretic and relaxation effects, that determine the concentration dependence of the conductivity. The former stems from the hydrodynamic interaction between ions and the latter does from the distortion of the ionic atmosphere under the applied electric field. Both effects contribute to the square-root limiting law of the electric conductivity and their coefficients were derived theoretically in the beginning of the 20th century.[2–5]

In addition to these two effects, the association between ions occurs in the concentrated electrolyte solutions when the dielectric constant of solvent is not sufficiently high.[12,13,16] A cation and an anion associate to form a neutral molecule called ion pair, which does not contribute to the electric conductivity. In the solvent of low dielectric constant, complicated behavior of the concentration dependence of the electric conductivity is sometimes observed and is attributed to higher order aggregates such as triple ions.[14]

We recently proposed a theory on the frequency-dependent electric conductivity of electrolyte solutions based on the generalized Langevin theory (hereafter called Paper I).[17] The random force on ionic currents is projected onto the ion pair distribution, whose time dependence is calculated by the Langevin equation. The static three- and four-body correlation functions are evaluated by the hypernetted-chain (HNC) integral equation,[18,19] without resorting to the factorization approximation frequently used in the mode-coupling theory (MCT).[18,20,21]

The numerical results presented in Paper I demonstrate that the theory is able to treat the effects of both long-range electrostatic correlation between ions and specific association of ions such as ion pair formation. However, since the hydrodynamic interaction between ions are totally neglected, the correct limiting law is not obtained by the theory in Paper I. We shall improve the theory to include the hydrodynamic interaction between ions in this work, and investigate its effects in the full concentration range.

The system we apply the theory is the aqueous solution of NaCl under ambient conditions. The aqueous solution of NaCl is a representative strong electrolyte solution in which ions are fully dissociated, and it has been a typical system to test the performance of theories on electrolyte solutions. However, microscopic theories and molecular dynamics (MD) simulations show that the radial distribution function between cation and anion has a high peak at the contact distance, suggesting the existence of the contact ion pair (CIP).[19,22–26]

There were theoretical calculations on the concentration dependence of the electric conductivity of NaCl in water, in which water was treated as the dielectric continuum. Good agreement between theory and experiment was demonstrated there. In these studies, however, the "hydrated" radii of ions are often employed under the assumption that ions are fully hydrated and the existence of CIP is completely excluded.[6,15,27] The difference between the structures used in continuum-solvent models and those obtained by microscopic studies was already pointed out by Dufrêche *et al.*[28] in

[a]Author to whom correspondence should be addressed. Electronic mail: tyama@nuce.nagoya-u.ac.jp.

 © 2009 American Institute of Physics

Downloaded 20 Jan 2010 to 133.6.32.53. Redistribution subject to AIP license or copyright; see http://jcp.aip.org/jcp/copyright.jsp

their theoretical study on the self-diffusion of ions. Although they considered several reasons to justify the use of effective radii, they did not perform calculations to support their arguments.

Our present work is devoted to the following two aims. The first one is to present the extension of our previous theory to include the hydrodynamic interaction between ions. The second one is to apply the theory to the aqueous solution of NaCl in order to make some contribution to resolving the discrepancy between the structure derived in microscopic ways and that used to reproduce the concentration dependence of the conductivity.

II. THEORY

The details of the theoretical derivations are summarized in the supporting information[29] and we shall here focus on the basic assumptions and the resulting formula. The system under consideration and the meanings of symbols are the same as those of Paper I unless they are mentioned explicitly in the text. It should be noted here that, since our present theoretical treatment is formulated as the diffusive limit of the ionic dynamics, the frequency dispersion of the conductivity due to the inertial motion or the in-cage vibration of ions observed in MD simulations[24,30] is not the target of our theory. Although these dynamics have been reported in the 100 GHz to the terahertz region, what we are focusing on are more slower phenomena in the megahertz to the gigahertz region.

A. Ionic current correlation function and conductivity

The Kubo–Green formula relates the time-correlation function of the electric current density with the frequency-dependent electric conductivity as[18,20,21]

$$\sigma(\nu) = \frac{1}{3k_BTV}\int_0^\infty dt e^{-2\pi i\nu t}\langle \mathbf{J}_{\mathrm{el}}(0)\cdot\mathbf{J}_{\mathrm{el}}(t)\rangle. \tag{1}$$

Hereafter we consider only the ionic currents as the source of the electric current as follows:

$$\mathbf{j}_{\mathrm{el}}(t) = \sum_\alpha z_\alpha \mathbf{j}_\alpha(t). \tag{2}$$

The contribution of ion α to the electric current is similarly given by

$$\sigma_\alpha(\nu) = \frac{z_\alpha}{3k_BTV}\int_0^\infty dt e^{-2\pi i\nu t}\langle \mathbf{J}_\alpha(0)\cdot\mathbf{J}_{\mathrm{el}}(t)\rangle, \tag{3}$$

and the transport number of cation in the binary electrolyte solution, denoted as t_+, is defined as

$$t_+ = \frac{\sigma_+(\nu=0)}{\sigma(\nu=0)}. \tag{4}$$

B. Projection onto ion pair distribution

In Paper I, the projection operator onto the instantaneous ion pair distribution is applied to the time propagator for the random force in order to extract the effect of ion pair distribution on the frequency-dependent electric conductivity. In this work, however, the same projection operator is applied to the time propagator for the *ionic current*, not that for the random force. The equivalence of the two formalisms is proven in the supporting information when the hydrodynamic interaction between ions is neglected.[29]

The equality for the time propagator for the ionic current leads to the expression for its time correlation function as

$$\begin{aligned}\langle j_{\alpha,z}e^{i\mathcal{L}t}j_{\gamma,z}\rangle &= \langle j_{\alpha,z}e^{i\mathcal{L}'t}j_{\gamma,z}\rangle \\ &+ \int_0^t d\tau\int_0^{t-\tau} d\tau'\langle j_{\alpha,z}e^{i\mathcal{L}'\tau'}i\mathcal{L}\mathcal{P}_1 e^{i\mathcal{L}(t-\tau-\tau')} \\ &\times\mathcal{P}_1 i\mathcal{L}e^{i\mathcal{L}'\tau}j_{\gamma,z}\rangle,\end{aligned} \tag{5}$$

where $\mathcal{L}' \equiv \mathcal{Q}_1\mathcal{L}\mathcal{Q}_1$. The proof of Eq. (5) is shown in the supporting information.[29]

In dense liquids, since the relaxation of the velocity of ions according to $e^{i\mathcal{L}'t}$ is faster than that of ion pair distribution, the second term is further approximated as

$$\begin{aligned}\langle j_{\alpha,z}e^{i\mathcal{L}t}j_{\gamma,z}\rangle &\simeq \langle j_{\alpha,z}e^{i\mathcal{L}'t}j_{\gamma,z}\rangle \\ &+ \sum_{\mu_1\sim\mu_4,\zeta_1\sim\zeta_4}\int\int\int\int d\mathbf{r}_1 d\mathbf{r}_2 d\mathbf{r}_3 d\mathbf{r}_4\left[\int_0^\infty d\tau'\langle j_{\alpha,z}e^{i\mathcal{L}'\tau'}i\mathcal{L}\delta\rho^{(2)}_{\mu_1\zeta_1}(\mathbf{r}_1)\rangle\right] \\ &\times\langle\delta\rho^{(2)}_{\mu_1\zeta_1}(\mathbf{r}_1)\delta\rho^{(2)}_{\mu_2\zeta_2}(\mathbf{r}_2)\rangle^{-1}\langle\delta\rho^{(2)}_{\mu_2\zeta_2}(\mathbf{r}_2)e^{i\mathcal{L}t}\delta\rho^{(2)}_{\mu_3\zeta_3}(\mathbf{r}_3)\rangle\langle\delta\rho^{(2)}_{\mu_3\zeta_3}(\mathbf{r}_3)\delta\rho^{(2)}_{\mu_4\zeta_4}(\mathbf{r}_4)\rangle^{-1}\left[\int_0^\infty d\tau\langle\delta\rho^{(2)}_{\mu_4\zeta_4}(\mathbf{r}_4)i\mathcal{L}e^{i\mathcal{L}'\tau}j_{\gamma,z}\rangle\right].\end{aligned} \tag{6}$$

It should be emphasized that the factorization in the rhs of Eq. (6) is not an approximation but just the result of the definition of projection operator. The approximation introduced in Eq. (6) is no other than the Markov approximation for the time correlation functions associated with $e^{i\mathcal{L}'t}$.

Downloaded 20 Jan 2010 to 133.6.32.53. Redistribution subject to AIP license or copyright; see http://jcp.aip.org/jcp/copyright.jsp

C. Dynamics of ion pair distribution

The time correlation function of the ion pair distribution is treated by the generalized Langevin theory we developed in the theories on the dynamic properties of electrolyte solutions.[17,31] The time correlation function of the pair distribution follows the Smoluchowski-type equation given by

$$\frac{\partial}{\partial t}\langle \delta\rho^{(2)}_{\alpha\gamma}(\mathbf{r}) e^{i\mathcal{L}t} \delta\rho^{(2)}_{\alpha'\gamma'}(\mathbf{r}')\rangle \simeq -\sum_{\mu\mu'\zeta\zeta'} \int d\mathbf{r}_1 \int d\mathbf{r}_2 \times \left[\int_0^\infty d\tau \langle \{i\mathcal{L}\delta\rho^{(2)}_{\alpha\gamma}(\mathbf{r})\} e^{i\mathcal{L}'\tau} \{i\mathcal{L}\delta\rho^{(2)}_{\mu\zeta}(\mathbf{r}_1)\}\rangle\right] \times \langle \delta\rho^{(2)}_{\mu\zeta}(\mathbf{r}_1)\delta\rho^{(2)}_{\mu'\zeta'}(\mathbf{r}_2)\rangle^{-1} \langle \delta\rho^{(2)}_{\mu'\zeta'}(\mathbf{r}_2) \times e^{i\mathcal{L}t}\delta\rho^{(2)}_{\alpha'\gamma'}(\mathbf{r}')\rangle. \tag{7}$$

Although the equation above looks similar to those in our previous theories,[17,31] it is different from them in that the former is on the *normal* time propagation of the pair distribution, whereas the latter is on the *projected* one.

D. Hydrodynamic interaction between two ions

The Oseen tensor is a popular approximation for the hydrodynamic interaction between molecules 1 and 2, which is given by

$$\int_0^\infty d\tau \langle \mathbf{v}_1 \otimes e^{i\mathcal{L}'\tau}\mathbf{v}_2\rangle = \frac{k_BT}{8\pi\eta r^3}[r^2\mathbf{1} + \mathbf{r}\otimes\mathbf{r}], \tag{8}$$

where $\mathbf{r}$ stands for the vector from molecule 1 to 2 and η denotes the shear viscosity of neat solvent. On the other hand, the self-correlation of the velocity of molecule 1 is given by

$$\int_0^\infty d\tau \langle \mathbf{v}_1 \otimes e^{i\mathcal{L}'\tau}\mathbf{v}_1\rangle = 3D_1\mathbf{1}, \tag{9}$$

where D_1 means the *bare* diffusion coefficient of the molecule 1.

The diffusion matrix for a pair of molecules must be positive definite. The approximation for the hydrodynamic interaction given by Eq. (8) satisfies the requirement only if the interionic distance is larger than $k_BT/4\pi\eta\sqrt{D_1D_2}$. We therefore modify the short range behavior of Eq. (8) as

$$\int_0^\infty d\tau \langle \mathbf{v}_1 \otimes e^{i\mathcal{L}'\tau}\mathbf{v}_2\rangle = \frac{k_BT}{8\pi\eta r^3}[r^2\mathbf{1} + \mathbf{r}\otimes\mathbf{r}] \times [1 - \mathrm{erfc}(\kappa_h r)], \tag{10}$$

where κ_h is determined by

$$\kappa_h = \frac{2\pi\eta\sqrt{D_1D_2\pi}}{k_BT}. \tag{11}$$

The ionic current correlation functions can be evaluated based on the approximation above, which is summarized in the supporting information.[29]

E. Conductivity and ion pair distribution

From the equations above and those in the supporting information,[29] the frequency-dependent conductivity is described in terms of the relaxation of ion pair distribution as

$$\sigma_0 - \sigma(\nu) = \delta\sigma_h + \delta\sigma_r(\nu), \tag{12}$$

as is in the theory of Altenberger and Friedman.[6]

The value of σ_0 is given by

$$\sigma_0 = \frac{1}{k_BT}\sum_\alpha \rho_\alpha z_\alpha^2 D_\alpha, \tag{13}$$

which is the low-concentration limiting law called the Nernst–Einstein equation.[1,18]

The effect of hydrodynamic interaction, denoted as $\delta\sigma_h$, stems from the velocity cross correlation in the first term of Eq. (6). It is explicitly given by

$$\delta\sigma_h = -\sum_{\alpha\gamma}\frac{2\rho_\alpha\rho_\gamma z_\alpha z_\gamma}{3\eta}\int_0^\infty dr r g_{\alpha\gamma}(r), \tag{14}$$

which is equivalent to the corresponding term in the theory of Altenberger and Friedman.[6] Equation (14) can be evaluated easily from the ion pair distribution to obtain $\delta\sigma_h$.

The contribution of the relaxation effect, denoted as $\delta\sigma_r(\nu)$, is described as

$$\delta\sigma_r(\nu) = \int_0^\infty dt e^{-2\pi i\nu t}\sum_{\alpha\gamma}\int d\mathbf{r}\,\phi_{\alpha\gamma}(\mathbf{r})\rho^{(2)}_{x,\alpha\gamma}(\mathbf{r},t), \tag{15}$$

where $\rho^{(2)}_{x,\alpha\gamma}(\mathbf{r})$ denotes the response of the ion pair distribution to the external electric field, whose time dependence is given by Eq. (7) as

$$\frac{\partial}{\partial t}\rho^{(2)}_{x,\alpha\gamma}(\mathbf{r},t) \simeq -\sum_{\mu\mu'\zeta\zeta'}\int d\mathbf{r}_1\int d\mathbf{r}_2 \times \left[\int_0^\infty d\tau \langle \{i\mathcal{L}\delta\rho^{(2)}_{\alpha\gamma}(\mathbf{r})\} e^{i\mathcal{L}'\tau}\{i\mathcal{L}\delta\rho^{(2)}_{\mu\zeta}(\mathbf{r}_1)\}\rangle\right] \times \langle \delta\rho^{(2)}_{\mu\zeta}(\mathbf{r}_1)\delta\rho^{(2)}_{\mu'\zeta'}(\mathbf{r}_2)\rangle^{-1}\rho^{(2)}_{x,\mu'\zeta'}(\mathbf{r}_2,t), \tag{16}$$

and its initial value is defined as

$$\rho^{(2)}_{x,\alpha\gamma}(\mathbf{r},t=0) = \int_0^\infty dt \langle \delta\rho^{(2)}_{\alpha\gamma}(\mathbf{r}) i\mathcal{L}e^{i\mathcal{L}'t}J_{el,z}\rangle. \tag{17}$$

The function that describes the coupling between the ion pair distribution and conductivity, denoted as $\phi_{\alpha\gamma}(\mathbf{r})$, is given by

$$\phi_{\alpha\gamma}(\mathbf{r}) = \frac{1}{k_BTV}\sum_{\mu\zeta}\int d\mathbf{r}' \langle \delta\rho^{(2)}_{\alpha\gamma}(\mathbf{r})\delta\rho^{(2)}_{\mu\zeta}(\mathbf{r}')\rangle^{-1}\rho^{(2)}_{x,\mu\zeta}(\mathbf{r}',t=0). \tag{18}$$

We need three steps to calculate $\delta\sigma_r(\nu)$ from the pair correlation functions. First one is the calculation of the initial value of $\rho^{(2)}_{x,\alpha\gamma}(\mathbf{r},t)$ by Eq. (17). Its time propagation is then performed according to Eq. (16) and is finally substituted into Eq. (15). The three- and four-body correlation functions that appear in Eqs. (16) and (17) are approximately evaluated as is described in the supporting information.[29]

Downloaded 20 Jan 2010 to 133.6.32.53. Redistribution subject to AIP license or copyright; see http://jcp.aip.org/jcp/copyright.jsp

Both Eqs. (14) and (15) are described as the integral over the distance between the pair of ions, so that they can be divided into the contributions of the ion pair distribution at various distances. The contribution of ion α to the electric conductivity is similarly given by

$$\sigma_{0,\alpha} - \sigma_{\alpha}(\nu) = \delta\sigma_{h,\alpha} + \delta\sigma_{r,\alpha}(\nu), \tag{19}$$

where $\sigma_{0,\alpha}$ is given by

$$\sigma_{0,\alpha} = \frac{\rho_{\alpha} z_{\alpha}^2 D_{\alpha}}{k_B T}, \tag{20}$$

and $\delta\sigma_{h,\alpha}$ is described as

$$\delta\sigma_{h,\alpha} = -\sum_{\gamma} \frac{2\rho_{\alpha}\rho_{\gamma} z_{\alpha} z_{\gamma}}{3\eta} \int_0^{\infty} dr r g_{\alpha\gamma}(r). \tag{21}$$

The relaxation term, $\delta\sigma_{r,\alpha}(\nu)$, is similarly given by

$$\delta\sigma_{r,\alpha}(\nu) = \int_0^{\infty} dt e^{-2\pi i \nu t} \sum_{\mu\zeta} \int d\mathbf{r} \phi_{\mu\zeta}^{(\alpha)}(\mathbf{r}) \rho_{x,\mu\zeta}^{(2)}(\mathbf{r},t),$$

$$\phi_{\mu\zeta}^{(\alpha)}(\mathbf{r}) = \frac{z_{\alpha}}{k_B T V} \sum_{\mu'\zeta'} \int d\mathbf{r}' \langle \delta\rho_{\mu\zeta}^{(2)}(\mathbf{r}) \delta\rho_{\mu'\zeta'}^{(2)}(\mathbf{r}') \rangle^{-1} \times \int_0^{\infty} dt \langle \delta\rho_{\mu'\zeta'}^{(2)}(\mathbf{r}) i\mathcal{L} e^{i\mathcal{L}' t} J_{\alpha,z} \rangle. \tag{22}$$

III. MODELS AND NUMERICAL METHODS

The system we consider is the aqueous solutions of NaCl. The temperature and pressure are 298 K and 1 bar, respectively, and the concentration of the salt is varied from 0.01 to 2 mol/kg. The densities of water and salt are taken from the literature.[32] The *bare* diffusion coefficients of ions are calculated from the limiting molar conductivity[32] and the shear viscosity of the solvent is also taken from the literature.[32] The concentration dependence of the bare diffusion coefficients and the shear viscosity is neglected.

The potential parameters employed are determined based on those proposed by Imai *et al.*[33] Although we first performed the calculations using their parameters, we found that the modification of parameters are necessary for the reasons described in the next section. The LJ parameters for ion-water and ion-ion interactions are those modified in order to reproduce the mean activity coefficient by the calculation using the dielectrically consistent reference interaction model (DRISM)/HNC integral equation theory.[19,22] In particular, different parameters are used for the ion-water and ion-ion interactions. The geometry and the potential parameters of water are the same as those of SPC/E,[34] except for the small Lennard-Jones (LJ) core on the hydrogen atom.

The static structures of the electrolyte solutions are calculated by the DRISM/HNC integral equation. The dielectric constant of the solvent at the finite concentration of the salt, which is required as the input parameter for the DRISM calculation, is taken from the dielectric relaxation spectra reported by Buchner *et al.*[35] The numerical method to solve the integral equation is the modified direct inversion in the iterative subspace one.[19,36] The linear grid is employed for the interatomic distance. The size of the grid is 0.05 Å and the cutoff radius is 204.8 Å. The mean activity coefficient of the electrolyte is obtained from the analytical expression of the chemical potential based on the HNC closure.[19]

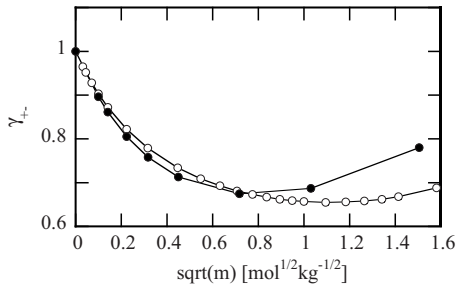

FIG. 1. The mean activity coefficient of NaCl in water is shown as the function of the square root of the concentration. The open and filled circles indicate the experimental and theoretical values, respectively.

The numerical algorithm for the relaxation of the pair distribution is the same as those in Paper I. Since the response of the pair distribution has the *p*-type symmetry, we need only to calculate its radial dependence, instead of the full three-dimensional distribution. The implicit method is used for the time integration of the equation of motion for the pair distribution. The size of the time grid is varied during the time integration as is described in Paper I. In the calculation of dynamics, the cutoff radius is 204.8 Å for the concentration below 0.1 mol/kg and 51.2 Å for the higher concentration. The effect of the different cutoff lengths is confirmed to be negligible at 0.1 mol/kg.

IV. RESULT AND DISCUSSION

A. Static structure and thermodynamic property

The potential parameters proposed by Imai *et al.* are determined in order to reproduce the concentration dependence of the mean activity coefficients by the DRISM/HNC theory. However, there remains a small disagreement between the experimental and theoretical values of the activity coefficients of NaCl in the present calculation for the following two reasons. First, the activity coefficients are calculated by Imai *et al.* based on the *molarity*,[37] whereas the conventional definition of the activity coefficient is given in terms of the *molality*. Second, the concentration dependence of the dielectric constant of the solvent in this work is different from that employed by them. Because both values were determined by the same experimental group and the value used in this work was published later than that employed by Imai *et al.*, we consider that the former is more reliable than the latter.

The parameters optimized by Imai *et al.* are the LJ diameter for the ion-ion interaction, keeping the coefficient of r^{-6} to that determined by the polarizability of ions. Therefore, we adjust the LJ diameter of Na^+ for ion-ion interaction, denoted as $\sigma_{LJ,+}$, in this work to reproduce the mean activity coefficient of NaCl below 1 mol/kg.

The mean activity coefficient thus obtained is plotted as the function of the concentration in Fig. 1. The experimental values[38] are exhibited together to demonstrate the good agreement at the concentration below 1 mol/kg. The value of

Downloaded 20 Jan 2010 to 133.6.32.53. Redistribution subject to AIP license or copyright; see http://jcp.aip.org/jcp/copyright.jsp

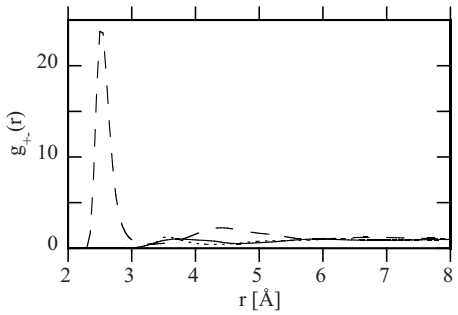

FIG. 2. The radial distribution functions between ions in the solution of 1 mol/kg are plotted. The solid, dashed, and dotted curves denote those between Na–Na, Na–Cl, and Cl–Cl, respectively.

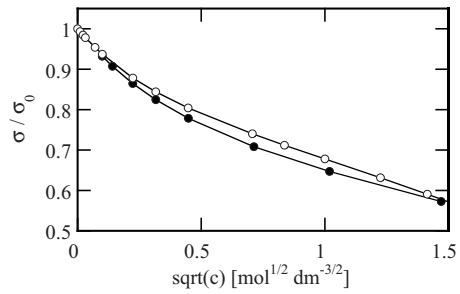

FIG. 3. The electric conductivity normalized to its limiting law value is exhibited against the square root of the concentration. The meanings of symbols are the same as those in Fig. 2.

$\sigma_{LJ,+}$ is 1.92 Å, whereas the original value proposed by Imai *et al.* is 1.86 Å. The LJ well-depth for the Na–Na interaction is changed to 0.275 kcal/mol in order to keep the coefficient of r^{-6} constant.

Figure 2 shows the radial distribution function between ions at 1 mol/kg. The most important feature to be noted is that there is a large peak in $g_{+-}(r)$ at the contact distance, which suggests the existence of the CIP. The coordination number of the counter ion determined by the integration of the radial distribution function is about 0.36.

It seems contradicting with the common sense that NaCl is a strong electrolyte in water, so that ion association does not occur. However, the large peak in $g_{+-}(r)$ at the contact distance is observed in other microscopic studies. First, the corresponding peak appears in the MD simulation irrespective of the potential parameters, although its height depends on the parameters.[23–26] The studies by the integral equation theories including solvent molecules also show the deep well at the contact distance in the potential of mean force between Na and Cl.[19,22]

In the diffraction experiments, the correlation between solute molecules is difficult to extract due to the small concentration of solute compared with that of solvent. For example, Ohtaki and Fukushima[39] demonstrated in the analysis of their x-ray diffraction experiments that the contribution of the Na–Cl contact peak to the total radial distribution function was about ten times smaller than that of O–O one even when the concentration was as high as 4.5 mol/kg and the coordination number of the counter ion is 0.3. Mancinelli *et al.*[40] measured the neutron diffraction of the aqueous solution of NaCl at various concentrations and extracted the site-site distribution functions by the combination with molecular simulation. Their radial distribution function between Na and Cl also had a large peak at the contact distance, which at least indicates that the existence of the CIP peak does not contradict with their neutron diffraction experiment. The height of the first peak of $g_{+-}(r)$ determined by them is 20–25 at 1 mol/kg, which is in good agreement with our present calculation.

One may consider that, although a large peak exists at the contact distance between a cation and an anion, it cannot be the ion pair in terms of electric conductivity due to the finite lifetime of the ion pair. In order to clarify whether it is true or not, the theory has to include the effect of finite lifetime of the ion pair. In addition, the contribution of the ion pair to the total change in the molar conductivity should be extracted by the theory. We would like to emphasize here that the development of our theory enabled us the above two. We already demonstrated in Paper I that the effect of the finite lifetime of the ion pair is taken into account in our theory. Equations (14) and (15) show that the contribution of CIP region is evaluated as the integral within the CIP region.

B. Concentration dependence of the conductivity

Figure 3 demonstrates the concentration dependence of the conductivity divided by its limiting values [Eq. (13)]. The theoretical values are plotted together with the experimental ones for comparison.[41] The agreement between the theory and experiment is good in the whole concentration region. In particular, the theory and experiment appear to converge to the same limiting behavior, reflecting that our theory obeys the correct limiting law. We believe that the agreement is good enough to consider that the physical mechanism our theoretical analysis shows reflect the real one.

In Fig. 4, the contributions of the electrophoretic and relaxation effects are separated and compared with the total one. The conductivity obtained by neglecting the relaxation effect, $\delta\sigma_r(\nu)$ in Eq. (12), is plotted to indicate the direct electrophoretic effect, and the value by neglecting the velocity cross correlation between two ions [Eq. (8)], is shown as the pure relaxation effect.

At a first glance, Eq. (12) appears to describe the loss of the conductivity from the limiting value as the sum of the electrophoretic and relaxation terms. It is true in the low concentration limit, as is the case of Debye–Onsager limiting

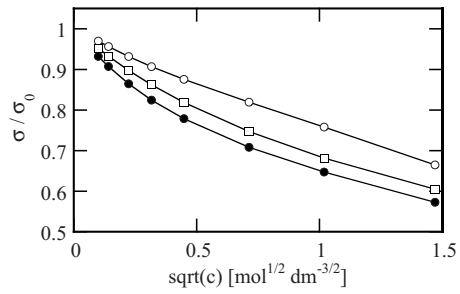

FIG. 4. The normalized electric conductivity obtained under various approximations are compared. The filled circles denote the results of the full theory and the open circles and squares do the values neglecting the hydrodynamic interaction and relaxation effect, respectively.

Downloaded 20 Jan 2010 to 133.6.32.53. Redistribution subject to AIP license or copyright; see http://jcp.aip.org/jcp/copyright.jsp

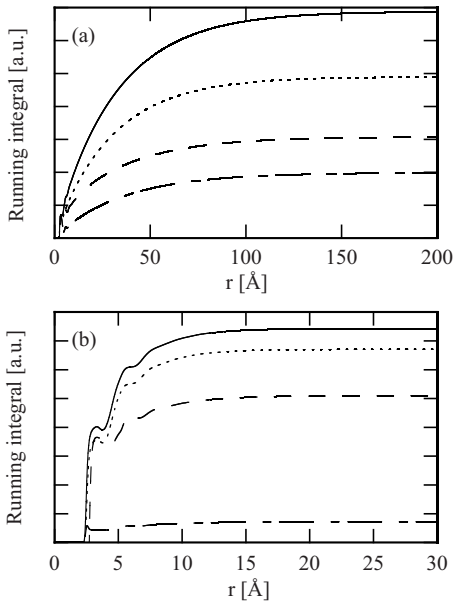

FIG. 5. The contributions of various interionic distances to the electric conductivity loss are plotted in the form of the running integral. Panels (a) and (b) demonstrate the results at 0.01 and 1 mol/kg, respectively. The solid curve stands for the results of the full theory, the dotted one does the direct hydrodynamic effect, and the dash-dotted and dashed ones do the relaxation effects with and without hydrodynamic interaction, respectively.

law. However, since the time dependence of the ion pair distribution is affected by the hydrodynamic interaction between ions, the effect of hydrodynamic interaction also enters in $\delta\sigma_r(\nu)$. As the result, the direct electrophoretic and pure relaxation effects strongly deviates from the additivity particularly in the higher concentration region. The reduction in the relaxation effect in the presence of the hydrodynamic interaction in the present work is in harmony with that reported by Dufrêche *et al.* in the case of self-diffusion of ions.[28]

In order to resolve this nonadditivity, the loss of the conductivity from the limiting law, $\sigma_0-\sigma(\nu=0)$, the direct electrophoretic effect, $\delta\sigma_h$, and the relaxation effects $\delta\sigma_r(\nu=0)$ with and without hydrodynamic interaction between different ions are divided as the sum of the contribution from different interionic distances. The results of 0.01 and 1 mol/kg are shown in Figs. 5(a) and 5(b), respectively, as the running integral from the origin.

In the case of 0.01 mol/kg, the contribution of the long-range distribution is dominant to the loss of conductivity, which indicates that the effects of ionic atmosphere are important as in the theory of Debye and Onsager. The functions for the relaxation effects with and without hydrodynamic interaction are parallel at large interionic distance, showing that the electrophoretic and relaxation effects from the long-range ion pair distribution are additive.

The situation is quite different in the case of 1 mol/kg. The contribution from the CIP region is about the half of the total effect and its magnitude little depends on the presence of the hydrodynamic interaction. Since the effect of hydrodynamic interaction is dominant in the CIP region as is shown in Fig. 5(b), the small dependence on the hydrodynamic interaction never means that it does not work in the

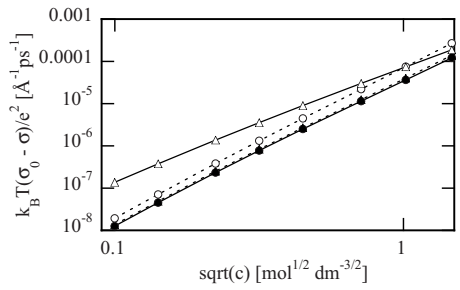

FIG. 6. The conductivity loss is plotted against the concentration. The filled circles and triangles denote the contribution from the CIP region obtained by the theories with and without the hydrodynamic interaction, respectively. The open circles and triangles do the static expectation [Eq. (30)] and the values of the full theory, respectively.

CIP region. A simple explanation is that since CIP is already bound to each other by strong interionic interaction, it does not contribute to the conductivity irrespective of the hydrodynamic interaction. In addition, the relaxation effect from the small interionic distance (<10 Å) is suppressed by the hydrodynamic interaction, which is considered to be due to the enhancement of the relaxation of ionic atmosphere caused by the hydrodynamic interaction.

Since the CIP region makes a remarkable contribution to the total conductivity loss, it is interesting to discuss the concentration dependence of the contribution of the CIP region. Figure 6 exhibits the CIP contributions with and without the hydrodynamic interaction. The total conductivity loss is also plotted for comparison. In addition, the contribution of CIP according to the static consideration defined as

$$\delta\sigma_p = \frac{z_+z_-\rho_+\rho_-(D_+ + D_-)}{k_BT}\int_{\mathrm{CIP}} 4\pi r^2 dr g_{+-}(r) \tag{23}$$

is shown together. The CIP region is defined here as $r<3.3$ Å, which is inside the first minimum of $g_{+-}(r)$ in the infinite dilution limit.

The magnitude of the CIP contribution is not affected by the presence of the hydrodynamic interaction between ions, as is demonstrated in Fig. 6. The fraction of the CIP contribution to the total conductivity loss increases with concentration, reflecting the relative decrease in the contribution of long-range pair distribution due to the decrease in the Debye screening length. Compared to the expectation of the static consideration, $\delta\sigma_p$, the dynamic result is smaller in all the concentration region. In the low-concentration region, the latter is by 0.7 times smaller than the former, which can be ascribed to the finite rate of the dissociation of CIP, as discussed in Paper I. The deviation between them increases in the higher concentration, which may reflect the many-body correlation between ions. The value of the static expectation exceeds the total conductivity loss at the concentration higher than 1 mol/kg, which indicates that the large coordination number of counter ion is compatible with large conductivity in concentrated electrolyte solutions.

One may consider that if there exists CIP in the aqueous solution of NaCl, it must be observed in the ultrasonic and dielectric relaxation spectra,[16] in contrast with the experimental observation that no relaxation assigned to CIP has been observed so far. In order to resolve the apparent con-

Downloaded 20 Jan 2010 to 133.6.32.53. Redistribution subject to AIP license or copyright; see http://jcp.aip.org/jcp/copyright.jsp

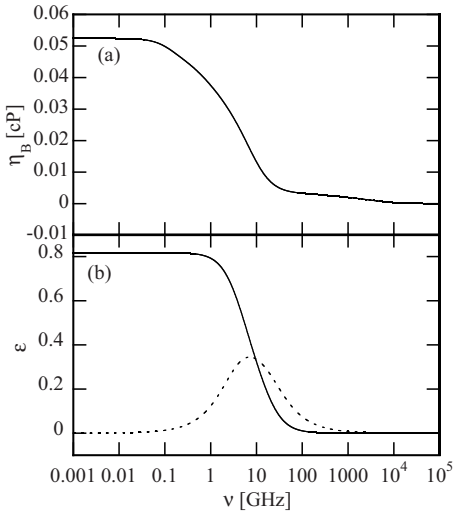

FIG. 7. Panels (a) and (b) demonstrate the frequency-dependent bulk viscosity and the dielectric susceptivity, respectively, as the function of frequency. In (b), the real and imaginary parts are shown by the solid and dotted curves, respectively.

tradiction with experiments, these relaxation spectra are calculated with the similar theories and the same static structure. The theory used to calculate the ultrasonic relaxation spectrum is proposed by us previously[31] and the dielectric relaxation spectrum is obtained from the frequency-dependent electric conductivity.

Figure 7(a) shows the frequency-dependent bulk viscosity arising from the ion pair distribution for 1 mol/kg solution. The amplitude of the relaxation is about two orders of magnitude smaller than the bulk viscosity of neat water. In addition, the main part of the relaxation is beyond 1 GHz, which is not accessible with the present experimental methods. Therefore our theoretical calculation is consistent with the experiments on the ultrasonic relaxation of the aqueous solution of NaCl.[42]

The dielectric relaxation spectrum for 1.0 mol/kg solution is shown in Fig. 7(b). The relaxation amplitude is about 0.8, which is in itself experimentally accessible. However, since the relaxation frequency is about 10 GHz, it overlaps with the large relaxation of water whose amplitude and frequency are about 70 and 20 GHz, respectively.[35] We consider that it is difficult to extract the ionic contribution to dielectric relaxation from the total dielectric response by the curve fitting procedure, because the response of water is also affected by the presence of ions. At higher concentration, 4.6 $\mathrm{mol/dm^3}$, the strong deviation from the Debye function is observed experimentally in the relaxation around 20 GHz,[35] which may be ascribed to the overlap with ionic contributions.

C. Effects of association strength

In this subsection, we further investigate the CIP contribution to the conductivity by artificially changing the height of the CIP peak of the radial distribution function between Na and Cl. The structures with different association strengths are prepared by modifying the LJ diameter of Na^+ for the ion-ion interaction from 1.86 to 2.04 Å. The radial distribution functions, $g_{+-}(r)$, are exhibited in Fig. 8. The height of the CIP peak decreases from 31 to 14 with increasing $\sigma_{LJ,+}$. In addition, the second peak at 4.4 Å slightly increases with the increase in $\sigma_{LJ,+}$.

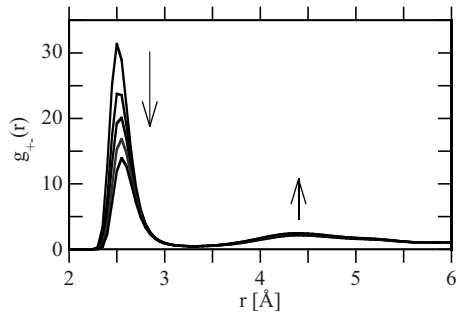

FIG. 8. The radial distribution functions between Na^+ and Cl^- with various values of $\sigma_{LJ,+}$ are exhibited. The arrows indicate the direction of change with increasing $\sigma_{LJ,+}$.

The number of counter ions within the CIP peak, defined as

$$N_{\mathrm{CIP}} \equiv \rho \int_{\mathrm{CIP}} 4\pi r^2 g_{+-}(r) dr, \tag{24}$$

is shown in Fig. 9. The *effective* association number is defined as

$$N_{\mathrm{CIP}}^{\mathrm{eff}} \equiv \frac{(\sigma_0 - \sigma) k_B T}{e^2 \rho (D_+ + D_-)}, \tag{25}$$

and plotted together. If the two-state model holds for the conductivity, the values of N_{CIP} and $N_{\mathrm{CIP}}^{\mathrm{eff}}$ agree with each other.

The association number, N_{CIP}, decreases with increasing $\sigma_{LJ,+}$ as is expected from $g_{+-}(r)$. Although $N_{\mathrm{CIP}}^{\mathrm{eff}}$ also decreases, however, its magnitude of the decrease is much smaller than that of N_{CIP}. It means that the conductivity does not increase so much as is expected from the decrease in the association number.

In order to resolve the difference between the changes of N_{CIP} and $N_{\mathrm{CIP}}^{\mathrm{eff}}$, the contribution of CIP peak to $N_{\mathrm{CIP}}^{\mathrm{eff}}$ is calculated in the same way as the previous subsection and plotted together in Fig. 9. The CIP contribution decreases in almost proportional to N_{CIP} and its change is larger than that of $N_{\mathrm{CIP}}^{\mathrm{eff}}$. We can therefore conclude that the small change in $N_{\mathrm{CIP}}^{\mathrm{eff}}$ is due to the cancellation of the decrease in the CIP contribu-

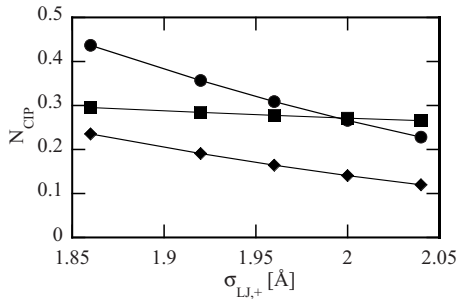

FIG. 9. N_{CIP} (circles) and $N_{\mathrm{CIP}}^{\mathrm{eff}}$ (squares), defined by Eqs. (24) and (25), respectively, are plotted as the function of $\sigma_{LJ,+}$. The diamonds stand for the contribution of CIP peak to $N_{\mathrm{CIP}}^{\mathrm{eff}}$.

Downloaded 20 Jan 2010 to 133.6.32.53. Redistribution subject to AIP license or copyright; see http://jcp.aip.org/jcp/copyright.jsp

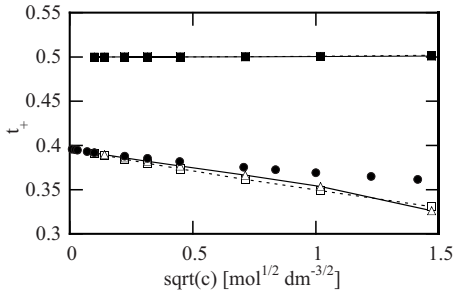

FIG. 10. The transport number of cation is plotted as the function of the square root of the concentration. The filled circles indicate the experimental values. The open triangles and squares do the values given by the full theory and direct hydrodynamic interaction, respectively. The filled triangles and squares correspond to the open ones except that they are calculated with the same *bare* diffusion coefficients for Na and Cl.

tion by the increase in the contribution of long-range interaction. The cancellation can be naturally understood in a sense, because the long-range Coulombic interaction is shielded by the distribution of the counter ion at shorter distance.

D. Transport number

Figure 10 exhibits the transport number of cation as the function of concentration. Both the theoretical and experimental[41] values are plotted for comparison. The decrease in t_+ with concentration is reproduced by the theory, although the theoretical magnitude of the decrease is by twice larger than the experimental one.

A theoretical analysis shows that the transport number does not depend on concentration without the hydrodynamic interaction between ions in our theory, as is the case of the theory of Altenberger and Friedman,[6] although the proof is omitted for brevity. The decrease in t_+ is thus ascribed to the hydrodynamic interaction. As is the case of conductivity, the hydrodynamic interaction can affect the transport number in two ways. One is through $\delta\sigma_{h,\alpha}$ given by Eq. (21) directly and the other is the indirect route through the relaxation of the ion pair distribution. Therefore we calculate the transport number without taking the relaxation effect into account in order to investigate the origin of the concentration dependence of the transport number. The result is plotted together in Fig. 10, which demonstrates that the direct route is essential.

We can expect from Eq. (21) that $\delta\sigma_{h,+}$ is approximately equal to $\delta\sigma_{h,-}$ for the following two reasons. First, the contribution of $g_{+-}(r)$, which is equal to both cation and anion, is dominant at small r due to the large population of cation-anion pair. Second, $g_{++}(r) \sim g_{--}(r)$ at large r because they are described well by the Debye–Hückel theory, so that the integrant for cation is nearly equal to that for anion. Provided that the decrease in current is equal for cation and anion, its effect is larger on the former, because the bare current without ion pair correlation of the former is smaller. In other words, our theory states that the concentration dependence of the transport number is caused by the asymmetry of the bare diffusion coefficient of ions.

Under the consideration above, we performed the calculation with the bare diffusion coefficients $D_+ = D_-$. The results with and without the relaxation effects are shown in Fig. 10. The transport numbers little deviate from 0.5, which justifies our theoretical analysis.

The statement that the concentration dependence of the transport number stems from the asymmetry of the bare diffusion coefficient is consistent with experimental results on aqueous solutions of various alkali halides.[41] The decrease in t_+ is larger for LiCl than for NaCl because the diffusivity of Li^+ is smaller than that of Na^+. The value of t_+ of KCl is close to 0.5 in all the concentration range because the limiting conductivities of cation and anion are close to each other. The increase in t_+ with concentration is observed in HCl whose t_+ is larger than 0.5, although it should be noted that the transport mechanism of proton is different from that of other cations.

E. Comparison with mode-coupling theory

The static structure used in the present calculation has a large CIP peak in the radial distribution function between cation and anion, as is observed in MD simulations and integral equation theories. The structure does not contradict with the x-ray and neutron diffraction experiments; Fig. 1 shows that the large CIP peak is consistent with the concentration dependence of the mean activity coefficient. In this work, we further demonstrate that the conductivity is also explained by the same structure and does not contradict with the ultrasonic and dielectric relaxation spectra. The theoretical analysis shows that the CIP peak actually contributes to about half of the conductivity loss at 1 mol/kg.

There are a number of theories on the electric conductivity of electrolyte solutions, in which the response of the pair distribution of ions is calculated as is performed in our theories. In most of these theories, the solvent is treated as the dielectric continuum and the correlation functions between ions are evaluated with the integral equation theory such as HNC or mean spherical approximation. The diameters of ions are treated as the fitting parameter to reproduce the concentration dependence of the conductivity in the concentration region up to 1 mol/kg. The diameters thus obtained are usually larger than the crystallographic ones. The effective diameters thus obtained are interpreted as those of the hydrated ions, not those of the bare ions. In particular, the distance between the cation and anion is restricted to be larger than the contact distance of bare ions.[6,15,27] The formation of CIP is therefore forbidden. The absence of CIP is usually attributed to the strong hydration of ions.

This subsection is devoted to the problem why the previous theories are not consistent with the structure which possesses the large CIP peak between cation and anion. The comparison is performed here with the MCT.[8–11,18,20,21] The same static pair correlation functions are employed for the MCT calculation in order to demonstrate the difference in the theory on dynamics. We have chosen MCT as the reference theory for following reasons. First, MCT is one of the popular theories on the dynamics of liquids and solutions. Second, the comparison is easy because our theory reduces to the MCT by neglecting the hydrodynamic interaction between ions and the introduction of the factorization approximation

Downloaded 20 Jan 2010 to 133.6.32.53. Redistribution subject to AIP license or copyright; see http://jcp.aip.org/jcp/copyright.jsp

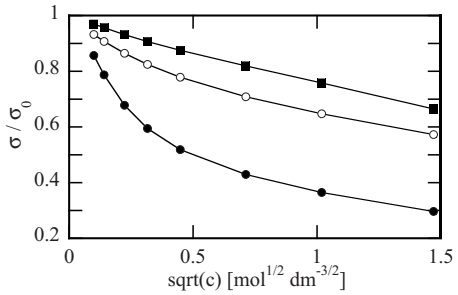

FIG. 11. The normalized conductivity from MCT (filled circles) is plotted against the square-root of the concentration, and compared with those from our theory with and without the hydrodynamic interaction (open circles and filled squares, respectively). The latter two are the same with those shown in Fig. 4.

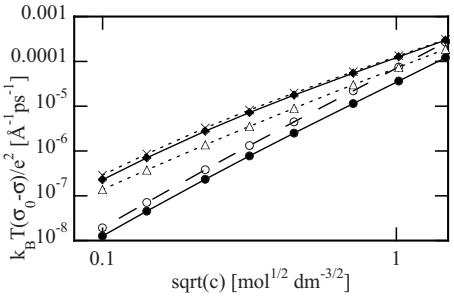

FIG. 13. The conductivity loss is plotted against the concentration. The total conductivity loss (open triangles), CIP contribution (filled circles), and static expectation (open circles) are the same as the corresponding values shown in Fig. 6 and compared with the total conductivity loss and its CIP contribution in MCT (crosses and filled diamonds, respectively).

for the three- and four-body correlation functions between ions. Third, as will be demonstrated later, the major discrepancy between our theory and MCT comes from the factorization approximation. Since the factorization approximation is often used by other theories that treat the response of the pair distribution, the problems of MCT due to the factorization approximation are common to other theories.

Figure 11 compares the concentration dependence of the conductivity obtained by the our theory and MCT. The results by neglecting the hydrodynamic interaction but still reserving the many-body correlation functions without resorting to the factorization approximation are also plotted. The last one is actually the same as the results of the relaxation effect without hydrodynamic interaction shown in Fig. 4. As is demonstrated in Fig. 11, the introduction of the factorization approximation strongly suppresses the conductivity.

The conductivity losses in these three theories are divided into the contributions of various interionic distances. The results at 0.01 mol/kg are plotted in Fig. 12, which clearly demonstrates that the large conductivity loss in MCT is exclusively attributed to the CIP region. The contribution of the long-range distribution is little affected by the factorization approximation, which exhibits that the factorization approximation works well for the long-range fluctuation of the ionic concentration.

The contribution of CIP region in MCT is plotted against the concentration in Fig. 13. The total conductivity loss is also shown for comparison. The conductivity loss comes exclusively from CIP region in MCT in all the concentration range studied here. The factorization approximation greatly enhances the conductivity loss from the CIP region especially in the low concentration region. Compared with the expectation from the static coordination number, Eq. (23), the CIP contribution in MCT is more than ten times larger than the static expectation at the lowest concentration studied here. In the low concentration region where many-body correlation is small, the effect of the interaction between a cation and an anion must be limited to these two ions. Therefore, we cannot justify the result of MCT as the low concentration behavior that the formation of CIP reduces the conductivity to the degree larger than the static expectation.

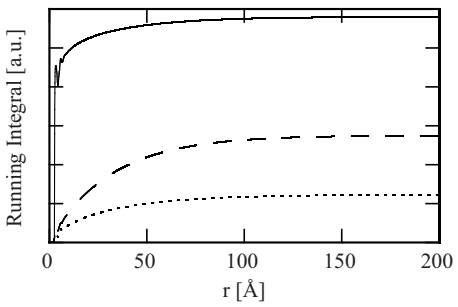

FIG. 12. The division of the conductivity loss into the contributions of various interionic distances is exhibited as the running integral. The function for MCT (solid curve) is compared with those for the theories with and without hydrodynamic interaction (dashed and dotted curves, respectively).

The error in the factorization approximation can be explained physically in the following way. The meaning of the factorization approximation for the time correlation function of the pair distribution is that a couple of ions move independently during the correlation time. However, since the ion pair is a couple of ions, which are bound to each other through the strong interionic interaction, the dynamics of these ions should be treated taking the binding into account.

In the theory on the conductivity of electrolyte solutions employing the factorization approximation, the distribution of the counter ion at the contact distance leads to the extremely large friction on the ionic current, which is not consistent with experiments. The counter ion must be excluded out of the CIP region by increasing the effective radii of ions in order to reproduce the concentration dependence of the conductivity by these theories. The absence of the CIP peak in the theoretical structure optimized for the concentration dependence of the conductivity can therefore be attributed to the error in the factorization approximation.

V. SUMMARY

We extended our previous theory on the electric conductivity of electrolyte solutions to include the effects of the hydrodynamic interaction between ions. The theory is applied to the aqueous solution of NaCl. The good agreement between the theoretical and experimental values is obtained.

The hydrodynamic and relaxation effects are additive in the dilute concentration region, whereas the hydrodynamic interaction suppresses the relaxation effect in the concentrated region. These two effects are divided into the contribution of different interionic distances. Their long range con-

Downloaded 20 Jan 2010 to 133.6.32.53. Redistribution subject to AIP license or copyright; see http://jcp.aip.org/jcp/copyright.jsp

tributions are additive, while the short range ones are not. Due to the dominance of the long range contribution, the hydrodynamic and relaxation effects are additive in the low concentration region. On the other hand, about half of the conductivity loss comes from the CIP region at 1 mol/kg. The magnitude of the CIP contribution is almost insensitive to the presence of the hydrodynamic interaction during all the concentration studied here, because the ions in CIP are bound to each other irrespective of the hydrodynamic interaction between them. The cancellation between the hydrodynamic and relaxation effects in the high concentration region is attributed to the CIP contribution. The CIP contribution is compared with the total conductivity loss and its static expectation [Eq. (23)]. The CIP contribution from the dynamic calculation is about 0.6–0.7 times smaller than the static expectation.

The concentration dependence of the transport number is obtained at the same time. The decrease in the transport number with concentration is qualitatively reproduced by the theory, although the quantitative agreement is not good. The decrease in the transport number of the cation is totally ascribed to the hydrodynamic interaction, and explained by the difference in the bare diffusion coefficients of the cation and anion.

Our present theory is compared with the results of MCT employing the same static correlation functions between ions. The conductivity loss given by MCT is much larger than that of our theory, which is ascribed to the factorization approximation used in MCT. The division into the contributions of different interionic ranges demonstrates that the overestimate of the conductivity loss is exclusively assigned to the CIP region.

Although our present theory reproduces the concentration dependence of the conductivity well, the agreement of the transport number is not so good. One reason for the discrepancy is the static structure. However, we consider that the static structure is not the principal reason for the discrepancy in the transport number, because the value of t_+ varies only slightly from 0.340 to 0.351 by changing $\sigma_{\mathrm{LJ},+}$ from 1.86 to 2.04 Å.

The second candidate is the approximation for the hydrodynamic interaction between ions, for which we employed the Oseen tensor approximation. The Oseen tensor approximation has the correct long-range asymptotic behavior, leading to the correct low-concentration limiting law. However, since the hydrodynamic Stokes–Einstein relationship does not hold for ions as small as Na^+, we have no reason to expect that the macroscopic hydrodynamics can be applied to the dynamics of solvent around the ion in the molecular scale. Since the hydrodynamic interaction is the principal factor that determines the concentration dependence of the transport number, we consider that the approximation for the hydrodynamic interaction is a main reason for the disagreement in the transport number.

The third possibility is the bare diffusion coefficient of ions. Although we assumed that the bare diffusion coefficients are constant, they may depend on the concentration of the electrolyte due to the modification of the solvent structure by ions. In order to resolve the latter two problems, we need to treat the dynamics of both solvent and solute at the same time, keeping the current densities as the slow variables. The treatment of the current of solvents around the solute is now under development[43,44] and we believe that this kind of study will be combined with the present theory to resolve the problems above.

ACKNOWLEDGMENTS

This work was partly supported by Grants-in-Aid from the Ministry of Education, Culture, Sports, Science and Technology of Japan (Grant No. 20740240). T.Y. is grateful to Dr. T. Imai (RIKEN) for the information on the parameter optimization for the RISM calculation of salt solutions.

[1] J. O'M. Bockris and A. K. N. Reddy, *Modern Electrochemistry* (Plenum, New York, 1970), Vol. 1.
[2] P. Debye and E. Hückel, Phys. Z. **24**, 305 (1923).
[3] L. Onsager, Phys. Z. **27**, 388 (1926).
[4] L. Onsager, Phys. Z. **28**, 277 (1927).
[5] L. Onsager and R. M. Fuoss, J. Phys. Chem. **36**, 2689 (1932).
[6] A. R. Altenberger and H. L. Friedman, J. Chem. Phys. **78**, 4162 (1983).
[7] O. Bernard, W. Kunz, P. Turq, and L. Blum, J. Phys. Chem. **96**, 3833 (1992).
[8] A. Chandra, R. Biswas, and B. Bagchi, J. Am. Chem. Soc. **121**, 4082 (1999).
[9] A. Chandra and B. Bagchi, J. Chem. Phys. **110**, 10024 (1999).
[10] A. Chandra and B. Bagchi, J. Chem. Phys. **112**, 1876 (2000).
[11] A. Chandra and B. Bagchi, J. Phys. Chem. B **104**, 9067 (2000).
[12] R. M. Fuoss and C. A. Kraus, J. Am. Chem. Soc. **55**, 476 (1933).
[13] R. M. Fuoss and C. A. Kraus, J. Am. Chem. Soc. **55**, 1019 (1933).
[14] R. M. Fuoss and C. A. Kraus, J. Am. Chem. Soc. **55**, 2387 (1933).
[15] J.-F. Dufrêche, O. Bernard, S. Durand-Vidal, and P. Turq, J. Phys. Chem. B **109**, 9873 (2005).
[16] Y. Marcus and G. Hefter, Chem. Rev. (Washington, D.C.) **106**, 4585 (2006).
[17] T. Yamaguchi, T. Matsuoka, and S. Koda, J. Chem. Phys. **127**, 234501 (2007).
[18] J.-P. Hansen and I. R. McDonald, *Theory of Simple Liquids*, 2nd ed. (Academic, London, 1990).
[19] F. Hirata, *Molecular Theory of Solvation* (Kluwer, Dordrecht, 2003).
[20] J. P. Boon and S. Yip, *Molecular Hydrodynamics* (McGraw-Hill, New York, 1980).
[21] U. Balucani and M. Zoppi, *Dynamics of the Liquid State* (Clarendon, Oxford, 1994).
[22] J. Perkyns and B. M. Pettitt, J. Chem. Phys. **97**, 7656 (1992).
[23] D. E. Smith and L. X. Dang, J. Chem. Phys. **100**, 3757 (1994).
[24] S. Chowdhuri and A. Chandra, J. Chem. Phys. **115**, 3732 (2001).
[25] M. Patra and M. Karttunen, J. Comput. Chem. **25**, 678 (2004).
[26] A. A. Chen and R. V. Pappu, J. Phys. Chem. B **111**, 6469 (2007).
[27] S. van Damme and J. Deconinck, J. Phys. Chem. B **111**, 5308 (2007).
[28] J.-F. Dufrêche, M. Jardat, P. Turq, and B. Bagchi, J. Phys. Chem. B **112**, 10264 (2008).
[29] See EPAPS Document No. E-JCPSA6-130-038909 for details of the theoretical calculations. For more information on EPAPS, see http://www.aip.org/pubservs/epaps.html.
[30] A. Chandra, D. Wei, and G. N. Patey, J. Chem. Phys. **99**, 2083 (1993).
[31] T. Yamaguchi, T. Matsuoka, and S. Koda, J. Chem. Phys. **126**, 144505 (2007).
[32] The Japanese Society of Chemistry, *Kagaku Binran Kisohen*, 5th ed. (Marubun, Tokyo, 2004).
[33] T. Imai, M. Kinoshita, and F. Hirata, Bull. Chem. Soc. Jpn. **73**, 1113 (2000).
[34] H. J. C. Berendsen, J. R. Grigera, and T. P. Straatsma, J. Phys. Chem. **91**, 6269 (1987).
[35] R. Buchner, G. T. Hefter, and P. M. May, J. Phys. Chem. A **103**, 1 (1999).
[36] A. Kovalenko, S. Ten-no, and F. Hirata, J. Comput. Chem. **20**, 928 (1999).
[37] T. Imai, private communication.
[38] W. J. Hamer and Y.-C. Wu, J. Phys. Chem. Ref. Data **1**, 1047 (1972).

Downloaded 20 Jan 2010 to 133.6.32.53. Redistribution subject to AIP license or copyright; see http://jcp.aip.org/jcp/copyright.jsp

[39] H. Ohtaki and N. Fukushima, J. Solution Chem. **21**, 23 (1992).
[40] R. Mancinelli, A. Botti, F. Bruni, M. A. Ricci, and A. K. Soper, J. Phys. Chem. B **111**, 13570 (2007).
[41] D. G. Miller, J. Phys. Chem. **70**, 2639 (1966).
[42] G. Kurtze and K. Tamm, Acustica **3**, 33 (1953).
[43] T. Yamaguchi, T. Matsuoka, and S. Koda, J. Chem. Phys. **123**, 034504 (2005).
[44] T. Yamaguchi, T. Matsuoka, and S. Koda, J. Mol. Liq. **134**, 1 (2007).

Downloaded 20 Jan 2010 to 133.6.32.53. Redistribution subject to AIP license or copyright; see http://jcp.aip.org/jcp/copyright.jsp